

Received:
19 January 2015

Revised:
25 March 2015

Accepted:
31 March 2015

© 2015 The Authors. Published by the British Institute of Radiology under the terms of the Creative Commons Attribution-NonCommercial 4.0 Unported License <http://creativecommons.org/licenses/by-nc/4.0/>, which permits unrestricted non-commercial reuse, provided the original author and source are credited.

Cite this article as:

Thorwarth D. Functional imaging for radiotherapy treatment planning: current status and future directions—a review. *Br J Radiol* 2015;88: 20150056.

ADVANCES IN RADIOTHERAPY SPECIAL FEATURE: REVIEW ARTICLE

Functional imaging for radiotherapy treatment planning: current status and future directions—a review

D THORWARTH, PhD

Section for Biomedical Physics, Department of Radiation Oncology, Eberhard Karls University Tübingen, Tübingen, Germany

Address correspondence to: Dr Daniela Thorwarth
E-mail: daniela.thorwarth@med.uni-tuebingen.de

ABSTRACT

In recent years, radiotherapy (RT) has been subject to a number of technological innovations. Today, RT is extremely flexible, allowing irradiation of tumours with high doses, whilst also sparing normal tissues from doses. To make use of these additional degrees of freedom, integration of functional image information may play a key role (i) for better staging and tumour detection, (ii) for more accurate RT target volume delineation, (iii) to assess functional information about biological characteristics and individual radiation resistance and (iv) to apply personalized dose prescriptions. In this article, we discuss the current status and future directions of different clinically available functional imaging modalities; CT, MRI, positron emission tomography (PET) as well as the hybrid imaging techniques PET/CT and PET/MRI and their potential for individualized RT.

Radiotherapy (RT) has, in the past two decades, been subject to a number of technological innovations. Modern RT techniques such as intensity-modulated RT, volumetric modulated arc therapy, as well as proton and heavy ion therapy are extremely flexible, benefiting from a high number of degrees of freedom in both the treatment planning process and in radiation delivery. As a consequence, in RT today, high levels of dose coverage of the tumour volume can be realized hand in hand with organ at risk sparing. Moreover, this flexibility gives room for escalating the radiation dose to more radioresistant areas of the gross tumour volume (GTV) with the aim of increasing tumour control probability without increasing the side effects of RT.

Modern functional imaging techniques, such as functional CT, MRI or positron emission tomography (PET) allow to visualize surrogates of a variety of pathophysiological characteristics of tumour tissue, such as metabolism, proliferation, hypoxia, perfusion etc. Consequently, integration of functional imaging seems to be very promising for individualized RT treatment planning.¹

Functional CT techniques such as dynamic contrast-enhanced CT (DCE-CT) as well as dynamic contrast-enhanced MRI (DCE-MRI) allow us to measure surrogates of tissue perfusion. Diffusion-weighted MRI (DW-MRI)

estimates the degrees of freedom that water molecules have to travel in tissue. Thus, in patients with cancer, DW-MRI is used to determine regions with abnormal extracellular space, which is used as an estimate of tumour cell density. PET imaging allows us to measure the specific uptake of radio-tracers and depending on the tracer used, can allow estimation of a number of different physiological properties of tumour tissue, such as metabolism, hypoxia or proliferation which are known to be key factors for cancer treatment.²

Consequently, integration of functional CT or MRI and molecular PET information to (re)direct radiation dose seems to be a powerful strategy to improve modern RT planning and to overcome biology-driven radiation resistance.^{2,3} In the past years, different strategies for using functional information have been proposed. First, additional complementary information from functional CT, MRI or PET imaging has been shown to improve target volume delineation in order to more accurately direct the radiation dose to the tumour region.²⁻⁴ Furthermore, higher radiation doses can be prescribed to a subvolume of the tumour, which is more radiation resistant as identified by functional imaging. This concept is called dose painting.⁵ Moreover, the functional imaging-guided increase in dose may be distributed inhomogeneously throughout the whole tumour volume according to activity distributions or, more generally, to parametric

maps derived from functional imaging using a dedicated prescription function.^{6,7}

In this article, the current status of functional imaging using CT, MRI and PET will be reviewed with respect to its prognostic value for RT outcome and to the possibility of potential integration into RT treatment planning. Furthermore, current developments and future directions that may be relevant for RT treatment adaptation in the future are discussed.

CT IMAGING TECHNIQUES

For several decades, CT has been the standard to base RT treatment planning and dose calculation on in order to achieve the highest dosimetric accuracy.⁸ Three-dimensional high-resolution imaging to estimate linear X-ray attenuation coefficients has become a major prerequisite for high-precision RT planning and delivery. Although, research on the use of other additional imaging techniques is currently evolving, there have also been major developments in CT during recent years. For example, fast and accurate iterative reconstruction techniques are now clinically available, which allow accurate quantitative imaging of mass densities even in the presence of metal implants.⁹

A recent CT technique with special technical requirements is dual-energy CT (DECT).¹⁰ DECT offers a more specific tissue classification¹¹ and therefore allows for more accurate Monte Carlo dose calculations in the RT planning process.^{12–14} This may be especially interesting in the advent of particle therapy such as proton or carbon ion treatment planning and the respective dose calculations. Several studies have described and controversially discussed the potential of DECT to reduce metal artefacts, which is also very important for classical X-ray-based RT.^{15–17}

Moreover, DCE-CT imaging allows us to estimate tissue perfusion by injecting iodine-based contrast agents in addition to repetitive CT imaging for approximately 40 s. Thus, DCE-CT has the potential to determine functional parameters such as blood flow, tissue perfusion and others from the contrast agent dynamics. For RT treatment planning, the availability of DCE-CT data can have enormous advantages as studies have shown that perfusion CT may improve the accuracy of RT target volume delineation.^{18–20} In addition, changes in perfusion parameters measured with MRI or CT during treatment have been shown to potentially give valuable information for monitoring therapy efficacy and success.²¹ A major advantage of using DCE-CT to estimate tissue perfusion lies in the linear relationship between signal intensity and contrast concentration compared with DCE-MRI, where signal-to-contrast conversion is very challenging.

A recently published study proposed a parametric method for automatically analysing perfusion information from volumetric DCE-CT data on a voxel basis in order to make this technology available as a biomarker for RT.²² The study showed that parametric voxel-based analysis of DCE-CT data resulted in greater accuracy and reliability in measuring changes in

perfusion CT-based kinetic metrics, which have the potential to be used as biomarkers in patients with brain metastasis.

DW-MRI, DCE-MRI AND MRS FOR RT OUTCOME PROGNOSIS AND TREATMENT PLANNING

In recent years, an increasing number of research projects have been initiated to explore the potential of DW-MRI, DCE-MRI and also MR spectroscopy (MRS) to assess their prognostic value, to improve RT treatment planning and delivery and to explore potential biomarkers for personalized RT in the future.

DCE-MRI—similarly to DCE-CT—allows us to assess the vascular properties of tissues by injecting a gadolinium-based contrast agent and acquiring a dynamic set of MR images.²³ Perfusion properties are then derived from the time-dependent signal by applying dedicated compartment models that are fitted to the signal curves. A recent study showed that by using DCE-MRI data, it was possible to identify subvolumes of brain metastases that were associated with therapy response.²⁴ In this study, the major component to determine response to therapy using principal component analysis was the area under the DCE curve. A number of different clinical studies have shown that DCE-MRI information has prognostic value with regard to RT outcome in head and neck cancer (HNC).^{25–27} In a study by Halle et al,²⁸ the prognostic impact of DCE-MRI parameters in cervical cancer acquired prior to radiochemotherapy combined with global gene expression data was explored. In this study, DCE-MRI was successfully correlated with a hypoxia gene signature that also showed prognostic impact in an independent validation cohort of 109 patients. The results of this project are a first step towards decrypting the molecular basis of an aggressive hypoxic phenotype and suggest the use of DCE-MRI to non-invasively identify patients with hypoxia-related chemoradioresistance.²⁹ Furthermore, it has been shown that DCE-MRI data can successfully be used for response assessment after completion of therapy.³⁰ However, acquisition and also analysis and interpretation of DCE-MRI data are technically extremely challenging. Also, the choice of the correct model to be used for kinetic analysis has to be made carefully.³¹

By contrast, DW-MRI offers a contrast-free method to assess the diffusion properties of water in tissue. This functional MRI method allows us to quantify voxel-based diffusion coefficients, more exactly, signal-derived maps of the apparent diffusion coefficient (ADC) that differ from one tissue to another. Thus, DW-MRI seems to be a powerful method when it comes to identifying the diffusion properties of a tumour mass. A recent histological study showed that the ADC signal value was significantly correlated with histological characteristics of HNC, such as cellularity, stromal component and nuclear–cytoplasmic ratio.³² Several studies have recently shown the prognostic potential of ADC to predict treatment outcome after RT in different tumour entities.^{33–36} In a recent Belgian study, the prognostic value of pre-treatment ADC in a large patient population with HNC was assessed and integrated into a multivariable prognostic model with the aim of estimating the individual patient's outcome prognosis.³⁷ The study revealed that pre-treatment ADC value derived from high *b*-values is an independent prognostic factor in HNC and increases the performance of

a multivariable prognostic model when used in addition with known clinical and radiological variables. Another study investigated texture analysis of ADC images in conjunction with multivariate analysis to identify pre-treatment imaging biomarkers.³⁸ By combining principal component analysis and texture analysis, ADC texture characteristics were identified, which seem to hold pre-treatment prognostic information, independent of known clinical prognostic factors. Further clinical trials confirmed the high value of DW-MRI for response assessment early after completion of RT.^{39–41}

A French group investigated the prognostic value of MRS imaging and assessed its impact on local tumour control in glioblastoma (GBM).^{42,43} Recently published results indicate that the lactate-to-N-acetyl-aspartate ratio (LNR) measured with MRS can discriminate between tumour-associated and normal LNR values with high sensitivity and specificity. Voxel areas presenting with low LNR values were spatially not colocalized with other MRI-defined volumes derived from contrast enhancement, central necrosis and fluid-attenuated inversion recovery abnormality before RT.⁴² As a consequence, pre-RT MRS in GBM seems to be able to detect tumour areas that are likely to relapse. Thus, MRS lactate imaging may be a future tool to define additional biological target volumes for dose painting.

PET FOR RT TARGET VOLUME DELINEATION AND ASSESSMENT OF FUNCTIONAL TUMOUR CHARACTERISTICS

PET has been established as a major source of metabolic and functional information for use during the RT planning process. PET imaging using the metabolic tracer fluorine-18 fludeoxyglucose (¹⁸F-FDG) is now a particularly important routine imaging modality not only for tumour grading and staging but also for accurate target volume delineation. Additional information on tumour geometry and extension may lead to better treatment outcomes. A number of studies so far have shown the benefit of ¹⁸F-FDG PET imaging for staging and definition of tumour extension.^{44,45} However, a study on 90 patients with oesophageal cancer reported that the value of ¹⁸F-FDG PET/CT for target volume delineation seems to be limited.⁴⁶ This study aimed at determining the proportion of locoregional recurrences that could have been prevented if RT planning for oesophageal cancer was based on PET/CT instead of CT. The result was negative. Further studies have assessed the prognostic value of dedicated PET-based parameters such as the maximum standardized uptake value (SUV) for overall survival and local tumour control.^{47–50} As a consequence, robust and accurate delineation of the ¹⁸F-FDG PET-positive tumour lesion is crucial.⁵¹ In recent years, a large number of studies and methodological research projects were carried out in order to develop and validate automatic and semi-automatic algorithms for accurate and robust delineation of RT target volumes based on ¹⁸F-FDG PET.^{51–62} Validation of new segmentation algorithms in terms of accuracy and robustness is of crucial importance for the potential clinical application of (semi-) automatic PET-based contouring.^{63,64} So far only a few clinical trials have been carried out in which dose escalation was prescribed on an ¹⁸F-FDG PET avid area inside the GTV.^{65–67}

Currently, two multicentre trials are testing the potential of redistributing the radiation dose to the metabolically most ¹⁸F-FDG PET avid part of the tumour in non-small-cell lung cancer (NSCLC)⁶⁵ and also in HNC.⁶⁶

PET imaging is not only beneficial for improving RT treatment planning in terms of target volume definition, it also has the potential to visualize functional and biological characteristics of tissue, such as tumour hypoxia. Tumour hypoxia was known for decades to be a key factor driving individual radiation resistance.^{68–70} As a consequence, non-invasive measurement of tumour hypoxia may be an important molecular marker for potential future RT adaptations.⁷¹ PET imaging allows for the detection of tumour hypoxia using different radiolabelled tracers, such as ¹⁸F-fluoromisonidazole (¹⁸F-FMISO),^{72–75} ¹⁸F-fluoroazomycin arabinoside (¹⁸F-FAZA)^{76–79} or ¹⁸F-flortanidazole (¹⁸F-HX4)^{80,81} among other less known tracers. A number of different studies have shown that a positive detection of tumour hypoxia using ¹⁸F-FMISO or ¹⁸F-FAZA PET is associated with a high risk of locoregional failure of chemoradiotherapy in NSCLC as well as in HNC.^{72,74,77} In addition, some studies have investigated the optimal time point of hypoxia imaging during the course of RT with the aim of identifying an ideal time point for potential therapy adaptation.^{73,74,77,79} Zips et al⁷⁴ analysed ¹⁸F-FMISO PET data for 25 patients with HNC examined before the start of RT as well as at Weeks 1, 2 and 5 during treatment. Similarly, Bollineni et al⁷⁷ report a study on six patients with NSCLC and six patients with HNC imaged with ¹⁸F-FAZA PET before chemo-RT and in treatment Weeks 1, 2 and 4. Both studies reported that hypoxia PET data acquired during the second week of treatment show the best correlation with observed treatment outcome and are thus most suitable and more reliable to base a potential treatment adaptation with, for example, dose painting on. However, quantitative hypoxia PET imaging is crucial for individualized RT alterations as well as for comparability of data in multicentre studies.⁸² So far, a variety of different concepts for the quantification of tumour hypoxia based on PET imaging have been used in different studies ranging from visual interpretation,⁷² tumour-to-background-based thresholding⁷⁹ and assessment of maximum or peak SUVs⁷⁴ to kinetic analysis of dynamically acquired hypoxia PET data.^{83–86} Here, a prerequisite for a potential future hypoxia-based RT intervention is a profound validation of hypoxia quantification measures based on PET. Furthermore, the different studies published so far all suffer from low patient numbers and a high variety of the respective imaging protocols, using image acquisition times ranging from 70⁸³ to 240 min⁷⁴ post injection (p.i.) of the tracer. Simulation experiments and the first clinical results have shown that image contrast improves with increasing time intervals between hypoxia tracer injection and PET image acquisition, which is owing to the slow diffusion of tracer in the tissue.^{87–89} Consequently, hypoxia PET image acquisition is recommended at 3–4 h p.i. for all nitroimidazole-based tracers. Direct comparison of the different clinically available hypoxia PET tracers has not been performed in a clinical setting so far. Two recent pre-clinical studies have compared the three tracers ¹⁸F-FMISO, ¹⁸F-FAZA and ¹⁸F-HX4; presenting highly inconclusive results about advantages and disadvantages and also the selection of an optimal tracer.^{90,91}

A further potentially very interesting PET tracer for RT adaptation and follow-up imaging is the proliferation marker ^{18}F -fluorothymidine (^{18}F -FLT).^{92,93} Initial clinical studies have shown that a change in ^{18}F -FLT uptake early during RT is a strong indicator for long-term outcome in HNC and NSCLC.^{92,93} ^{18}F -FLT PET may thus be a potential imaging biomarker to guide personalized patient management and treatment modifications during an early phase of treatment.

For other tumour entities, which physiologically do not present with increased glucose metabolism, such as prostate, new tracers are currently being developed to improve diagnosis and therapy. Recently, a highly specific tracer for the diagnosis of prostate tumours, the prostate-specific membrane antigen (PSMA) ligand (^{68}Ga)HBED-CC-PSMA was investigated.⁹⁴ Initial clinical studies using PSMA PET show very promising results in terms of a high sensitivity and specificity of PSMA PET for the identification of intraprostatic tumour foci, which would be a prerequisite for PET-based focal dose escalation in prostate cancer.⁹⁵ For RT target volume delineation in brain tumours, studies using amino acid PET tracers, such as ^{18}F -fluoro-ethyl-tyrosine PET or carbon-11 methionine PET have shown the potential to visualize tumour areas that do not seem to be detected *via* MRI and could therefore yield additional, complementary information.^{96–98}

HYBRID IMAGING MODALITIES AND MULTIPARAMETRIC FUNCTIONAL IMAGING

In addition to combined PET/CT⁹⁹ that has been the clinical standard for approximately 15 years now, new hybrid imaging technologies such as PET/MRI¹⁰⁰ have been developed in the past few years. In contrast to PET/CT, combined PET/MRI is still a matter of technological and also clinical research.¹⁰⁰ However, hybrid imaging modalities allow acquisition of two or more molecular, functional and anatomical image data sets either at the same time or successively in the same patient position. As a consequence, these scanners have the potential to be used for assessing different functional or biological characteristics of a tumour with only one examination, which might be highly interesting for RT personalization in the near future. Multiparametric functional imaging including new methodologies for large-scale data handling and analysis is an evolving field in RT research. A number of studies have investigated common features and correlations between different functional imaging modalities with the aim of increasing the accuracy in target volume delineation^{101–103} or detection of regions with increased radiation resistance.^{104–106}

Houweling et al¹⁰² have investigated whether ^{18}F -FDG PET and DW-MRI identify the same or different targets for dose escalation in the GTV of patients with HNC. The study found that these two imaging modalities contain different information, resulting in different RT targets, which hints at the complementary nature of the measured biological information. Groenendaal et al¹⁰³ developed a logistic regression model for voxel-by-voxel prediction of prostate tumour presence, validated *via* pathology. The model defines different risk levels for tumour presence, which were then used as a basis for improved tumour delineations for focal boost therapy. Another study by

van Elmpt et al¹⁰⁴ analysed differences in vasculature properties within NSCLC tumours measured by DCE-CT and metabolic information from ^{18}F -FDG PET/CT. In this study, no direct correlation was observed between ^{18}F -FDG PET and DCE-CT. Lambrecht et al¹⁰⁶ investigated the use of ^{18}F -FDG PET/CT before, during and after chemo-RT and DW-MRI before chemo-RT for the prediction of pathological response in patients with rectal cancer. The results of this study showed that the combination of different time points and different imaging modalities increased the specificity of the response assessment during and after chemo-RT. Similarly, Iizuka et al¹⁰⁵ showed that a combination of ADC and ^{18}F -FDG SUV was a better predictor for disease progression in NSCLC than one imaging modality alone. In analogy to dose painting concepts proposed for one single modality, more complex methods have been developed to base individualized RT treatment planning on multiparametric functional imaging information.¹⁰⁷

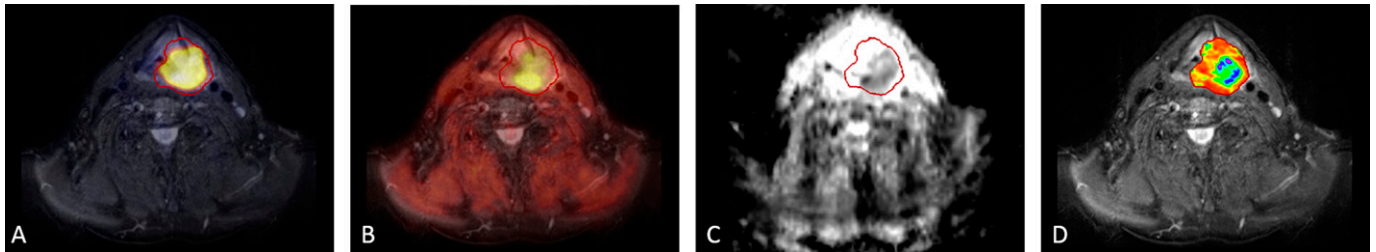
Figure 1 shows an example of a patient with HNC presenting with multiparametric functional imaging information before the start of RT. This patient has been examined with combined PET/MR in addition to PET/CT, yielding ^{18}F -FDG and ^{18}F -FMISO PET data as well as anatomical MRI and also functional DW- and DCE-MRI.

A recently evolving field in functional imaging research for RT is *radiomics*.^{108,109} Radiomics stands for the high-throughput extraction of a large amount of quantitative features from medical images, providing a comprehensive quantification of the tumour phenotype, yielding potentially complementary information to other sources such as demographics, pathology or genomics. In a large recent study, Aerts et al¹⁰⁹ applied a large number of quantitative image features to perform a radiomics analysis quantifying tumour image intensity, shape and texture, which are extracted from CT images of patients with HNC and patients with NSCLC. The study suggests that radiomics identifies general prognostic information, which may have a strong clinical impact to improve decision support in RT and cancer treatment in general.

REQUIREMENTS FOR THE USAGE OF FUNCTIONAL IMAGING IN RADIOTHERAPY

Integration of functional imaging in RT treatment planning requires special features in terms of image acquisition, quality and geometrical accuracy. For both functional imaging modalities, PET and MRI, a major pre-requisite for reproducible and robust image quality that can be safely taken into account during treatment planning is functional image acquisition in a dedicated RT treatment position.^{3,110} Consequentially, PET and MRI should be performed on a flat table top, using vacuum mattresses and thermoplastic mask systems for patient fixation in exactly the same position as during fractionated RT treatment. If necessary, dedicated coil set-ups enabling image acquisition with those additional hardware components in the field of view may be used for MRI.³ In the special case of combined PET/MR, dedicated PET- and MR-compatible positioning aids are required.¹¹¹ However, if imaging in RT position is not possible or in the presence of anatomical changes, dedicated methods for deformable image registration (DIR) are necessary

Figure 1. Multiparametric functional imaging of a 57-year-old male patient with head and neck cancer. (a) Fluorine-18 fludeoxyglucose positron emission tomography (PET) overlaid to anatomical T_2 weighted MRI, (b) combined fluorine-18 fluoromisonidazole PET/MRI acquired 4 h post injection, (c) apparent diffusion coefficient map derived from diffusion-weighted MRI and (d) perfusion map showing the distribution of the parameter K_{trans} derived *via* kinetic analysis from dynamic contrast-enhanced MRI inside the tumour volume. The radiotherapy gross tumour volume is outlined in each image slice.



to fuse functional imaging information on a voxel basis to the RT planning CT.^{112,113} However, DIR is still a matter of research, and dedicated algorithms are only available in research software because careful clinical validation of DIR methods is still lacking. When PET imaging is used for RT target delineation or treatment planning of dose painting, the accuracy of quantitative PET information is crucial. The quality of PET data depends on a number of different factors, such as the image acquisition protocol, image reconstruction settings and also the technical characteristics of the imaging system.^{114–117} Consequently, PET data used for RT planning needs to be acquired and analysed in a standardized way. Also, for the integration of (functional) MRI data into RT treatment planning, dedicated aspects in terms of patient positioning and image acquisition are required for a robust integration of the imaging data into the treatment planning process.³ Two recent studies have investigated the geometric accuracy and the level of reproducibility in functional DW-MRI.^{118,119} They found that DW-MRI can present with substantial geometric distortions¹¹⁸ and also low levels of reproducibility when comparing repeated

examinations.¹¹⁹ Both factors are crucial for functional image-guided high-precision RT.

CONCLUSION

Functional imaging with CT, PET, MRI or hybrid imaging modalities offer a variety of possibilities to detect and visualize functional and biological processes related to tumour pathophysiology and radiation sensitivity. While initial results are promising, as discussed in this review, much research is still necessary in this emerging field of RT. However, functional image-guided RT has the potential to advance today's RT towards personalized medicine, with the realistic aim of improving cancer treatment in the near future.

FUNDING

DT is supported by the European Research Council, Starting Grant number. 335367.

ACKNOWLEDGMENTS

Thanks to Sara Leibfarth for help with the figure. Emma Wilson is acknowledged for proof reading of the manuscript.

REFERENCES

- Bentzen SM, Gregoire V. Molecular imaging-based dose painting: a novel paradigm for radiation therapy prescription. *Semin Radiat Oncol* 2011; **21**: 101–10. doi: [10.1016/j.semradonc.2010.10.001](https://doi.org/10.1016/j.semradonc.2010.10.001)
- Nestle U, Weber W, Hentschel M, Grosu AL. Biological imaging in radiation therapy: role of positron emission tomography. *Phys Med Biol* 2009; **54**: R1–25. doi: [10.1088/0031-9155/54/1/R01](https://doi.org/10.1088/0031-9155/54/1/R01)
- van der Heide UA, Houweling AC, Groenendaal G, Beets-Tan RG, Lambin P. Functional MRI for radiotherapy dose painting. *Magn Reson Imaging* 2012; **30**: 1216–23. doi: [10.1016/j.mri.2012.04.010](https://doi.org/10.1016/j.mri.2012.04.010)
- Lagendijk JJ, Raaymakers BW, Van den Berg CA, Moerland MA, Philippens ME, van Vulpen M. MR guidance in radiotherapy. *Phys Med Biol* 2014; **59**: R349–69. doi: [10.1088/0031-9155/59/21/R349](https://doi.org/10.1088/0031-9155/59/21/R349)
- Bentzen SM. Theragnostic imaging for radiation oncology: dose-painting by numbers. *Lancet Oncol* 2005; **6**: 112–17. doi: [10.1016/S1470-2045\(05\)01737-7](https://doi.org/10.1016/S1470-2045(05)01737-7)
- Thorwarth D, Geets X, Paiusco M. Physical radiotherapy treatment planning based on functional PET/CT data. *Radiother Oncol* 2010; **96**: 317–24. doi: [10.1016/j.radonc.2010.07.012](https://doi.org/10.1016/j.radonc.2010.07.012)
- Thorwarth D, Eschmann SM, Paulsen F, Alber M. Hypoxia dose painting by numbers: a planning study. *Int J Radiat Oncol Biol Phys* 2007; **68**: 291–300. doi: [10.1016/j.ijrobp.2006.11.061](https://doi.org/10.1016/j.ijrobp.2006.11.061)
- Newbold K, Partridge M, Cook G, Sohaib SA, Charles-Edwards E, Rhys-Evans P, et al. Advanced imaging applied to radiotherapy planning in head and neck cancer: a clinical review. *Br J Radiol* 2006; **79**: 554–61. doi: [10.1259/bjr/48822193](https://doi.org/10.1259/bjr/48822193)
- Meyer E, Raupach R, Lell M, Schmidt B, Kachelrieß M. Frequency split metal artifact reduction (FSMAR) in computed tomography. *Med Phys* 2012; **39**: 1904–16. doi: [10.1118/1.3691902](https://doi.org/10.1118/1.3691902)
- Johnson TR. Dual-energy CT: general principles. *AJR Am J Roentgenol* 2012; **199**(5 Suppl.): S3–8. doi: [10.2214/AJR.12.9116](https://doi.org/10.2214/AJR.12.9116)
- Johnson TR, Krauss B, Sedlmair M, Grasruck M, Bruder H, Morhard D, et al. Material differentiation by dual energy CT: initial experience. *Eur Radiol* 2007; **17**: 1510–17. doi: [10.1007/s00330-006-0517-6](https://doi.org/10.1007/s00330-006-0517-6)
- Landry G, Reniers B, Granton PV, van Rooijen B, Beaulieu L, Wildberger JE, et al. Extracting atomic numbers and

- electron densities from a dual source dual energy CT scanner: experiments and a simulation model. *Radiother Oncol* 2011; **100**: 375–9. doi: [10.1016/j.radonc.2011.08.029](https://doi.org/10.1016/j.radonc.2011.08.029)
13. Bazalova M, Carrier JF, Beaulieu L, Verhaegen F. Tissue segmentation in Monte Carlo treatment planning: a simulation study using dual-energy CT images. *Radiother Oncol* 2008; **86**: 93–8. doi: [10.1016/j.radonc.2007.11.008](https://doi.org/10.1016/j.radonc.2007.11.008)
 14. Yamada S, Ueguchi T, Ogata T, Mizuno H, Oghihara R, Koizumi M, et al. Radiotherapy treatment planning with contrast-enhanced computed tomography: feasibility of dual-energy virtual unenhanced imaging for improved dose calculations. *Radiat Oncol* 2014; **9**: 168. doi: [10.1186/1748-717x-9-168](https://doi.org/10.1186/1748-717x-9-168)
 15. Bamberg F, Dierks A, Nikolaou K, Reiser MF, Becker CR, Johnson TR. Metal artifact reduction by dual energy computed tomography using monoenergetic extrapolation. *Eur Radiol* 2011; **21**: 1424–9. doi: [10.1007/s00330-011-2062-1](https://doi.org/10.1007/s00330-011-2062-1)
 16. Guggenberger R, Winklhofer S, Osterhoff G, Wanner GA, Fortunati M, Andreisek G, et al. Metallic artefact reduction with monoenergetic dual-energy CT: systematic *ex vivo* evaluation of posterior spinal fusion implants from various vendors and different spine levels. *Eur Radiol* 2012; **22**: 2357–64. doi: [10.1007/s00330-012-2501-7](https://doi.org/10.1007/s00330-012-2501-7)
 17. Kuchenbecker S, Faby S, Sawall S, Lell M, Kachelrieß M. Dual energy CT: how well can pseudo-monochromatic imaging reduce metal artifacts? *Med Phys* 2015; **42**: 1023–36. doi: [10.1118/1.4905106](https://doi.org/10.1118/1.4905106)
 18. Jensen NK, Mulder D, Lock M, Fisher B, Zener R, Beech B, et al. Dynamic contrast enhanced CT aiding gross tumor volume delineation of liver tumors: an interobserver variability study. *Radiother Oncol* 2014; **111**: 153–7. doi: [10.1016/j.radonc.2014.01.026](https://doi.org/10.1016/j.radonc.2014.01.026)
 19. van Elmpt W, Zegers CM, Das M, De Ruyscher D. Imaging techniques for tumour delineation and heterogeneity quantification of lung cancer: overview of current possibilities. *J Thorac Dis* 2014; **6**: 319–27. doi: [10.3978/j.issn.2072-1439.2013.08.62](https://doi.org/10.3978/j.issn.2072-1439.2013.08.62)
 20. Korporaal JG, van den Berg CA, Groenendaal G, Moman MR, van Vulpen M, van der Heide UA. The use of probability maps to deal with the uncertainties in prostate cancer delineation. *Radiother Oncol* 2010; **94**: 168–72. doi: [10.1016/j.radonc.2009.12.023](https://doi.org/10.1016/j.radonc.2009.12.023)
 21. Kallehaug J, Nielsen T, Haack S, Peters DA, Mohamed S, Fokdal L, et al. Voxelwise comparison of perfusion parameters estimated using dynamic contrast enhanced (DCE) computed tomography and DCE-magnetic resonance imaging in locally advanced cervical cancer. *Acta Oncol* 2013; **52**: 1360–8. doi: [10.3109/0284186x.2013.813637](https://doi.org/10.3109/0284186x.2013.813637)
 22. Coolens C, Driscoll B, Chung C, Shek T, Gorjizadeh A, Ménard C, et al. Automated voxel-based analysis of volumetric dynamic contrast-enhanced CT data improves measurement of serial changes in tumor vascular biomarkers. *Int J Radiat Oncol Biol Phys* 2015; **91**: 48–57. doi: [10.1016/j.ijrobp.2014.09.028](https://doi.org/10.1016/j.ijrobp.2014.09.028)
 23. Jain R. Measurements of tumor vascular leakiness using DCE in brain tumors: clinical applications. *NMR Biomed* 2013; **26**: 1042–9. doi: [10.1002/nbm.2994](https://doi.org/10.1002/nbm.2994)
 24. Farjam R, Tsien CI, Lawrence TS, Cao Y. DCE-MRI defined subvolumes of a brain metastatic lesion by principle component analysis and fuzzy-c-means clustering for response assessment of radiation therapy. *Med Phys* 2014; **41**: 011708. doi: [10.1118/1.4842556](https://doi.org/10.1118/1.4842556)
 25. Wang P, Popovtzer A, Eisbruch A, Cao Y. An approach to identify, from DCE MRI, significant subvolumes of tumors related to outcomes in advanced head-and-neck cancer. *Med Phys* 2012; **39**: 5277–85. doi: [10.1118/1.4737022](https://doi.org/10.1118/1.4737022)
 26. Shukla-Dave A, Lee NY, Jansen JF, Thaler HT, Stambuk HE, Fury MG, et al. Dynamic contrast-enhanced magnetic resonance imaging as a predictor of outcome in head-and-neck squamous cell carcinoma patients with nodal metastases. *Int J Radiat Oncol Biol Phys* 2012; **82**: 1837–44. doi: [10.1016/j.ijrobp.2011.03.006](https://doi.org/10.1016/j.ijrobp.2011.03.006)
 27. Ng SH, Lin CY, Chan SC, Yen TC, Liao CT, Chang JT, et al. Dynamic contrast-enhanced MR imaging predicts local control in oropharyngeal or hypopharyngeal squamous cell carcinoma treated with chemoradiotherapy. *PLoS One* 2013; **8**: e72230. doi: [10.1371/journal.pone.0072230](https://doi.org/10.1371/journal.pone.0072230)
 28. Halle C, Andersen E, Lando M, Aarnes EK, Hasvold G, Holden M, et al. Hypoxia-induced gene expression in chemoradioresistant cervical cancer revealed by dynamic contrast-enhanced MRI. *Cancer Res* 2012; **72**: 5285–95. doi: [10.1158/0008-5472.CAN-12-1085](https://doi.org/10.1158/0008-5472.CAN-12-1085)
 29. Andersen EK, Hole KH, Lund KV, SundfØr K, Kristensen GB, Lyng H, et al. Pharmacokinetic parameters derived from dynamic contrast enhanced MRI of cervical cancers predict chemoradiotherapy outcome. *Radiother Oncol* 2013; **107**: 117–22. doi: [10.1016/j.radonc.2012.11.007](https://doi.org/10.1016/j.radonc.2012.11.007)
 30. Intven M, Reerink O, Philippens ME. Dynamic contrast enhanced MR imaging for rectal cancer response assessment after neo-adjuvant chemoradiation. *J Magn Reson Imaging* Aug 2014. Epub ahead of print. doi:[10.1002/jmri.24718](https://doi.org/10.1002/jmri.24718)
 31. Kallehaug JF, Tanderup K, Duan C, Haack S, Pedersen EM, Lindegaard JC, et al. Tracer kinetic model selection for dynamic contrast-enhanced magnetic resonance imaging of locally advanced cervical cancer. *Acta Oncol* 2014; **53**: 1064–72. doi: [10.3109/0284186x.2014.937879](https://doi.org/10.3109/0284186x.2014.937879)
 32. Driessen JP, Caldas-Magalhaes J, Janssen LM, Pameijer FA, Kooij N, Terhaar CH, et al. Diffusion-weighted MR imaging in laryngeal and hypopharyngeal carcinoma: association between apparent diffusion coefficient and histologic findings. *Radiology* 2014; **272**: 456–63. doi: [10.1148/radiol.14131173](https://doi.org/10.1148/radiol.14131173)
 33. Tshering Vogel DW, Zbaeren P, Geretschlaeger A, Vermathen P, De Keyzer F, Thoeny HC. Diffusion-weighted MR imaging including bi-exponential fitting for the detection of recurrent or residual tumour after (chemo)radiotherapy for laryngeal and hypopharyngeal cancers. *Eur Radiol* 2013; **23**: 562–9. doi: [10.1007/s00330-012-2596-x](https://doi.org/10.1007/s00330-012-2596-x)
 34. Galbán S, Lemasson B, Williams TM, Li F, Heist KA, Johnson TD, et al. DW-MRI as a biomarker to compare therapeutic outcomes in radiotherapy regimens incorporating temozolomide or gemcitabine in glioblastoma. *PLoS One* 2012; **7**: e35857. doi: [10.1371/journal.pone.0035857](https://doi.org/10.1371/journal.pone.0035857)
 35. Vandecaveye V, De Keyzer F, Nuyts S, Deraedt K, Dirix P, Hamaekers P, et al. Detection of head and neck squamous cell carcinoma with diffusion weighted MRI after (chemo)radiotherapy: correlation between radiologic and histopathologic findings. *Int J Radiat Oncol Biol Phys* 2007; **67**: 960–71. doi: [10.1016/j.ijrobp.2006.09.020](https://doi.org/10.1016/j.ijrobp.2006.09.020)
 36. Noij DP, Pouwels PJ, Ljumanovic R, Knol DL, Doornaert P, de Bree R, et al. Predictive value of diffusion-weighted imaging without and with including contrast-enhanced magnetic resonance imaging in image analysis of head and neck squamous cell carcinoma. *Eur J Radiol* 2015; **84**: 108–16. doi: [10.1016/j.ejrad.2014.10.015](https://doi.org/10.1016/j.ejrad.2014.10.015)
 37. Lambrecht M, Van Calster B, Vandecaveye V, De Keyzer F, Roebben I, Hermans R, et al. Integrating pretreatment diffusion weighted MRI into a multivariable prognostic model for head and neck squamous cell carcinoma. *Radiother Oncol* 2014; **110**: 429–34. doi: [10.1016/j.radonc.2014.01.004](https://doi.org/10.1016/j.radonc.2014.01.004)
 38. Brynolfsson P, Nilsson D, Henriksson R, Hauksson J, Karlsson M, Garpebring A, et al. ADC texture—an imaging biomarker for high-grade glioma? *Med Phys* 2014; **41**: 101903. doi: [10.1118/1.4894812](https://doi.org/10.1118/1.4894812)

39. Liu L, Wu N, Ouyang H, Dai JR, Wang WH. Diffusion-weighted MRI in early assessment of tumour response to radiotherapy in high-risk prostate cancer. *Br J Radiol* 2014; **87**: 20140359. doi: [10.1259/bjr.20140359](https://doi.org/10.1259/bjr.20140359)
40. Chen Y, Liu X, Zheng D, Xu L, Hong L, Xu Y, et al. Diffusion-weighted magnetic resonance imaging for early response assessment of chemoradiotherapy in patients with nasopharyngeal carcinoma. *Magn Reson Imaging* 2014; **32**: 630–7. doi: [10.1016/j.mri.2014.02.009](https://doi.org/10.1016/j.mri.2014.02.009)
41. Padhani AR, Koh DM. Diffusion MR imaging for monitoring of treatment response. *Magn Reson Imaging Clin N Am* 2011; **19**: 181–209. doi: [10.1016/j.mric.2010.10.004](https://doi.org/10.1016/j.mric.2010.10.004)
42. Deviers A, Ken S, Filleron T, Rowland B, Laruelo A, Catalaa I, et al. Evaluation of the lactate-to-N-acetyl-aspartate ratio defined with magnetic resonance spectroscopic imaging before radiation therapy as a new predictive marker of the site of relapse in patients with glioblastoma multiforme. *Int J Radiat Oncol Biol Phys* 2014; **90**: 385–93. doi: [10.1016/j.ijrobp.2014.06.009](https://doi.org/10.1016/j.ijrobp.2014.06.009)
43. Laprie A, Catalaa I, Cassol E, McKnight TR, Berchery D, Marre D, et al. Proton magnetic resonance spectroscopic imaging in newly diagnosed glioblastoma: predictive value for the site of postradiotherapy relapse in a prospective longitudinal study. *Int J Radiat Oncol Biol Phys* 2008; **70**: 773–81. doi: [10.1016/j.ijrobp.2007.10.039](https://doi.org/10.1016/j.ijrobp.2007.10.039)
44. Mac Manus MP, Everitt S, Bayne M, Ball D, Plumridge N, Binns D, et al. The use of fused PET/CT images for patient selection and radical radiotherapy target volume definition in patients with non-small cell lung cancer: results of a prospective study with mature survival data. *Radiother Oncol* 2013; **106**: 292–8. doi: [10.1016/j.radonc.2012.12.018](https://doi.org/10.1016/j.radonc.2012.12.018)
45. Mak D, Corry J, Lau E, Rischin D, Hicks RJ. Role of FDG-PET/CT in staging and follow-up of head and neck squamous cell carcinoma. *Q J Nucl Med Mol Imaging* 2011; **55**: 487–99.
46. Muijs CT, Beukema JC, Woutersen D, Mul VE, Berveling MJ, Pruijm J, et al. Clinical validation of FDG-PET/CT in the radiation treatment planning for patients with oesophageal cancer. *Radiother Oncol* 2014; **113**: 188–92. doi: [10.1016/j.radonc.2014.10.016](https://doi.org/10.1016/j.radonc.2014.10.016)
47. Castaldi P, Rufini V, Bussu F, Micciché F, Dinapoli N, Autorino R, et al. Can “early” and “late”¹⁸F-FDG PET-CT be used as prognostic factors for the clinical outcome of patients with locally advanced head and neck cancer treated with radio-chemotherapy? *Radiother Oncol* 2012; **103**: 63–8. doi: [10.1016/j.radonc.2012.03.001](https://doi.org/10.1016/j.radonc.2012.03.001)
48. Hentschel M, Appold S, Schreiber A, Abolmaali N, Abramjuk A, Dörr W, et al. Early FDG PET at 10 or 20 Gy under chemoradiotherapy is prognostic for locoregional control and overall survival in patients with head and neck cancer. *Eur J Nucl Med Mol Imaging* 2011; **38**: 1203–11. doi: [10.1007/s00259-011-1759-3](https://doi.org/10.1007/s00259-011-1759-3)
49. Horne ZD, Clump DA, Vargo JA, Shah S, Beriwal S, Burton SA, et al. Pretreatment SUVmax predicts progression-free survival in early-stage non-small cell lung cancer treated with stereotactic body radiation therapy. *Radiat Oncol* 2014; **9**: 41. doi: [10.1186/1748-717X-9-41](https://doi.org/10.1186/1748-717X-9-41)
50. Carvalho S, Leijenaar RT, Velazquez ER, Oberije C, Parmar C, van Elmpt W, et al. Prognostic value of metabolic metrics extracted from baseline positron emission tomography images in non-small cell lung cancer. *Acta Oncol* 2013; **52**: 1398–404. doi: [10.3109/0284186x.2013.812795](https://doi.org/10.3109/0284186x.2013.812795)
51. Doll C, Duncker-Rohr V, Rucker G, Mix M, MacManus M, De Ruyscher D, et al. Influence of experience and qualification on PET-based target volume delineation. When there is no expert—ask your colleague. *Strahlenther Onkol* 2014; **190**: 555–62. doi: [10.1007/s00066-014-0644-y](https://doi.org/10.1007/s00066-014-0644-y)
52. Shepherd T, Teras M, Beichel RR, Boellaard R, Bruynooghe M, Dicken V, et al. Comparative study with new accuracy metrics for target volume contouring in PET image guided radiation therapy. *IEEE Trans Med Imaging* 2012; **31**: 2006–24. doi: [10.1109/TMI.2012.2202322](https://doi.org/10.1109/TMI.2012.2202322)
53. Hapdey S, Edet-Sanson A, Gouel P, Martin B, Modzelewski R, Baron M, et al. Delineation of small mobile tumours with FDG-PET/CT in comparison to pathology in breast cancer patients. *Radiother Oncol* 2014; **112**: 407–12. doi: [10.1016/j.radonc.2014.08.005](https://doi.org/10.1016/j.radonc.2014.08.005)
54. Berthon B, Marshall C, Evans M, Spezi E. Evaluation of advanced automatic PET segmentation methods using nonspherical thin-wall inserts. *Med Phys* 2014; **41**: 022502. doi: [10.1118/1.4863480](https://doi.org/10.1118/1.4863480)
55. McGurk RJ, Bowsher J, Lee JA, Das SK. Combining multiple FDG-PET radiotherapy target segmentation methods to reduce the effect of variable performance of individual segmentation methods. *Med Phys* 2013; **40**: 042501. doi: [10.1118/1.4793721](https://doi.org/10.1118/1.4793721)
56. Werner-Wasik M, Nelson AD, Choi W, Arai Y, Faulhaber PF, Kang P, et al. What is the best way to contour lung tumors on PET scans? Multiobserver validation of a gradient-based method using a NSCLC digital PET phantom. *Int J Radiat Oncol Biol Phys* 2012; **82**: 1164–71. doi: [10.1016/j.ijrobp.2010.12.055](https://doi.org/10.1016/j.ijrobp.2010.12.055)
57. Wanet M, Lee JA, Weynand B, De Bast M, Poncelet A, Lacroix V, et al. Gradient-based delineation of the primary GTV on FDG-PET in non-small cell lung cancer: a comparison with threshold-based approaches, CT and surgical specimens. *Radiother Oncol* 2011; **98**: 117–25. doi: [10.1016/j.radonc.2010.10.006](https://doi.org/10.1016/j.radonc.2010.10.006)
58. Geets X, Lee JA, Bol A, Lonneux M, Grégoire V. A gradient-based method for segmenting FDG-PET images: methodology and validation. *Eur J Nucl Med Mol Imaging* 2007; **34**: 1427–38. doi: [10.1007/s00259-006-0363-4](https://doi.org/10.1007/s00259-006-0363-4)
59. Schaefer A, Kremp S, Hellwig D, Rube C, Kirsch CM, Nestle U. A contrast-oriented algorithm for FDG-PET-based delineation of tumour volumes for the radiotherapy of lung cancer: derivation from phantom measurements and validation in patient data. *Eur J Nucl Med Mol Imaging* 2008; **35**: 1989–99. doi: [10.1007/s00259-008-0875-1](https://doi.org/10.1007/s00259-008-0875-1)
60. Hatt M, Cheze le Rest C, Descourt P, Dekker A, De Ruyscher D, Oellers M, et al. Accurate automatic delineation of heterogeneous functional volumes in positron emission tomography for oncology applications. *Int J Radiat Oncol Biol Phys* 2010; **77**: 301–8. doi: [10.1016/j.ijrobp.2009.08.018](https://doi.org/10.1016/j.ijrobp.2009.08.018)
61. Hatt M, Cheze le Rest C, Turzo A, Roux C, Visvikis D. A fuzzy locally adaptive Bayesian segmentation approach for volume determination in PET. *IEEE Trans Med Imaging* 2009; **28**: 881–93. doi: [10.1109/TMI.2008.2012036](https://doi.org/10.1109/TMI.2008.2012036)
62. Ford EC, Kinahan PE, Hanlon L, Alessio A, Rajendran J, Schwartz DL, et al. Tumor delineation using PET in head and neck cancers: threshold contouring and lesion volumes. *Med Phys* 2006; **33**: 4280–8. doi: [10.1118/1.2361076](https://doi.org/10.1118/1.2361076)
63. Axente M, He J, Bass CP, Sundaresan G, Zweit J, Williamson JF, et al. An alternative approach to histopathological validation of PET imaging for radiation therapy image-guidance: a proof of concept. *Radiother Oncol* 2014; **110**: 309–16. doi: [10.1016/j.radonc.2013.12.017](https://doi.org/10.1016/j.radonc.2013.12.017)
64. Schinagl DA, Span PN, van den Hoogen FJ, Merx MA, Slootweg PJ, Oyen WJ, et al. Pathology-based validation of FDG PET segmentation tools for volume assessment of lymph node metastases from head and neck cancer. *Eur J Nucl Med Mol Imaging* 2013; **40**: 1828–35. doi: [10.1007/s00259-013-2513-9](https://doi.org/10.1007/s00259-013-2513-9)
65. van Elmpt W, De Ruyscher D, van der Salm A, Lakeman A, van der Stoep J,

- Emans D, et al. The PET-boost randomised phase II dose-escalation trial in non-small cell lung cancer. *Radiother Oncol* 2012; **104**: 67–71. doi: [10.1016/j.radonc.2012.03.005](https://doi.org/10.1016/j.radonc.2012.03.005)
66. Heukelom J, Hamming O, Bartelink H, Hoebers F, Giralto J, Herlestam T, et al. Adaptive and innovative radiation treatment for improving cancer treatment outcome (ARTFORCE); a randomized controlled phase II trial for individualized treatment of head and neck cancer. *BMC Cancer* 2013; **13**: 84. doi: [10.1186/1471-2407-13-84](https://doi.org/10.1186/1471-2407-13-84)
67. Madani I, Duprez F, Boterberg T, Van de Wiele C, Bonte K, Deron P, et al. Maximum tolerated dose in a phase I trial on adaptive dose painting by numbers for head and neck cancer. *Radiother Oncol* 2011; **101**: 351–5. doi: [10.1016/j.radonc.2011.06.020](https://doi.org/10.1016/j.radonc.2011.06.020)
68. Gray LH, Conger AD, Ebert M, Hornsey S, Scott OC. The concentration of oxygen dissolved in tissues at the time of irradiation as a factor in radiotherapy. *Br J Radiol* 1953; **26**: 638–48. doi: [10.1259/0007-1285-26-312-638](https://doi.org/10.1259/0007-1285-26-312-638)
69. Thomlinson RH, Gray LH. The histological structure of some human lung cancers and the possible implications for radiotherapy. *Br J Cancer* 1955; **9**: 539–49. doi: [10.1038/bjc.1955.55](https://doi.org/10.1038/bjc.1955.55)
70. Nordmark M, Overgaard M, Overgaard J. Pretreatment oxygenation predicts radiation response in advanced squamous cell carcinoma of the head and neck. *Radiother Oncol* 1996; **41**: 31–9. doi: [10.1016/S0167-8140\(96\)91811-3](https://doi.org/10.1016/S0167-8140(96)91811-3)
71. Horsman MR, Mortensen LS, Petersen JB, Busk M, Overgaard J. Imaging hypoxia to improve radiotherapy outcome. *Nat Rev Clin Oncol* 2012; **9**: 674–87. doi: [10.1038/nrclinonc.2012.171](https://doi.org/10.1038/nrclinonc.2012.171)
72. Rischin D, Hicks RJ, Fisher R, Binns D, Corry J, Porceddu S, et al; Trans-Tasman Radiation Oncology Group Study 98.02. Prognostic significance of [18F]-misonidazole positron emission tomography-detected tumor hypoxia in patients with advanced head and neck cancer randomly assigned to chemoradiation with or without tirapazamine: a sub-study of Trans-Tasman Radiation Oncology Group Study 98.02. *J Clin Oncol* 2006; **24**: 2098–104. doi: [10.1200/jco.2005.05.2878](https://doi.org/10.1200/jco.2005.05.2878)
73. Bittner MI, Wiedenmann N, Bucher S, Hentschel M, Mix M, Weber WA, et al. Exploratory geographical analysis of hypoxic subvolumes using 18F-MISO-PET imaging in patients with head and neck cancer in the course of primary chemoradiotherapy. *Radiother Oncol* 2013; **108**: 511–16. doi: [10.1016/j.radonc.2013.06.012](https://doi.org/10.1016/j.radonc.2013.06.012)
74. Zips D, Zöphel K, Abolmaali N, Perrin R, Abramjuk A, Haase R, et al. Exploratory prospective trial of hypoxia-specific PET imaging during radiochemotherapy in patients with locally advanced head-and-neck cancer. *Radiother Oncol* 2012; **105**: 21–8. doi: [10.1016/j.radonc.2012.08.019](https://doi.org/10.1016/j.radonc.2012.08.019)
75. Hendrickson K, Phillips M, Smith W, Peterson L, Krohn K, Rajendran J. Hypoxia imaging with [F-18] FMISO-PET in head and neck cancer: potential for guiding intensity modulated radiation therapy in overcoming hypoxia-induced treatment resistance. *Radiother Oncol* 2011; **101**: 369–75. doi: [10.1016/j.radonc.2011.07.029](https://doi.org/10.1016/j.radonc.2011.07.029)
76. Servagi-Vernat S, Differding S, Hanin FX, Labar D, Bol A, Lee JA, et al. A prospective clinical study of ¹⁸F-FAZA PET-CT hypoxia imaging in head and neck squamous cell carcinoma before and during radiation therapy. *Eur J Nucl Med Mol Imaging* 2014; **41**: 1544–52. doi: [10.1007/s00259-014-2730-x](https://doi.org/10.1007/s00259-014-2730-x)
77. Bollineni VR, Koole MJ, Pruijm J, Brouwer CL, Wiegman EM, Groen HJ, et al. Dynamics of tumor hypoxia assessed by 18F-FAZA PET/CT in head and neck and lung cancer patients during chemoradiation: possible implications for radiotherapy treatment planning strategies. *Radiother Oncol* 2014; **113**: 198–203. doi: [10.1016/j.radonc.2014.10.010](https://doi.org/10.1016/j.radonc.2014.10.010)
78. Bollineni VR, Kerner GS, Pruijm J, Steenbakkens RJ, Wiegman EM, Koole MJ, et al. PET imaging of tumor hypoxia using 18F-fluoroazomycin arabinoside in stage III-IV non-small cell lung cancer patients. *J Nucl Med* 2013; **54**: 1175–80. doi: [10.2967/jnumed.112.115014](https://doi.org/10.2967/jnumed.112.115014)
79. Mortensen LS, Johansen J, Kallehauge J, Primdahl H, Busk M, Lassen P, et al. FAZA PET/CT hypoxia imaging in patients with squamous cell carcinoma of the head and neck treated with radiotherapy: results from the DAHANCA 24 trial. *Radiother Oncol* 2012; **105**: 14–20. doi: [10.1016/j.radonc.2012.09.015](https://doi.org/10.1016/j.radonc.2012.09.015)
80. Zegers CM, van Elmpt W, Wierds R, Reymen B, Sharifi H, Öllers MC, et al. Hypoxia imaging with [¹⁸F]HX4 PET in NSCLC patients: defining optimal imaging parameters. *Radiother Oncol* 2013; **109**: 58–64. doi: [10.1016/j.radonc.2013.08.031](https://doi.org/10.1016/j.radonc.2013.08.031)
81. Zegers CM, van Elmpt W, Reymen B, Even AJ, Troost EG, Öllers MC, et al. *In vivo* quantification of hypoxic and metabolic status of NSCLC tumors using [18F]HX4 and [18F]FDG-PET/CT imaging. *Clin Cancer Res* 2014; **20**: 6389–97. doi: [10.1158/1078-0432.ccr-14-1524](https://doi.org/10.1158/1078-0432.ccr-14-1524)
82. Thureau S, Chaumet-Riffaud P, Modzelewski R, Fernandez P, Tessonnier L, Vervueren L, et al. Interobserver agreement of qualitative analysis and tumor delineation of 18F-fluoromisonidazole and 3'-deoxy-3'-18F-fluorothymidine PET images in lung cancer. *J Nucl Med* 2013; **54**: 1543–50. doi: [10.2967/jnumed.112.118083](https://doi.org/10.2967/jnumed.112.118083)
83. Verwer EE, Bahce I, van Velden FH, Yaqub M, Schuit RC, Windhorst AD, et al. Parametric methods for quantification of 18F-FAZA kinetics in non-small cell lung cancer patients. *J Nucl Med* 2014; **55**: 1772–7. doi: [10.2967/jnumed.114.141846](https://doi.org/10.2967/jnumed.114.141846)
84. Verwer EE, van Velden FH, Bahce I, Yaqub M, Schuit RC, Windhorst AD, et al. Pharmacokinetic analysis of [18F]FAZA in non-small cell lung cancer patients. *Eur J Nucl Med Mol Imaging* 2013; **40**: 1523–31. doi: [10.1007/s00259-013-2462-3](https://doi.org/10.1007/s00259-013-2462-3)
85. Wang W, Lee NY, Georgi JC, Narayanan M, Guillem J, Schöder H, et al. Pharmacokinetic analysis of hypoxia (18F)-fluoromisonidazole dynamic PET in head and neck cancer. *J Nucl Med* 2010; **51**: 37–45. doi: [10.2967/jnumed.109.067009](https://doi.org/10.2967/jnumed.109.067009)
86. Thorwarth D, Eschmann SM, Scheiderbauer J, Paulsen F, Alber M. Kinetic analysis of dynamic 18F-fluoromisonidazole PET correlates with radiation treatment outcome in head-and-neck cancer. *BMC Cancer* 2005; **5**: 152. doi: [10.1186/1471-2407-5-152](https://doi.org/10.1186/1471-2407-5-152)
87. Abolmaali N, Haase R, Koch A, Zips D, Steinbach J, Baumann M, et al. Two or four hour [¹⁸F]FMISO-PET in HNSCC. When is the contrast best? *Nuklearmedizin* 2011; **50**: 22–7. doi: [10.3413/nukmed-00328-10-07](https://doi.org/10.3413/nukmed-00328-10-07)
88. Mönnich D, Troost EG, Kaanders JH, Oyen WJ, Alber M, Thorwarth D. Modelling and simulation of [18F]fluoromisonidazole dynamics based on histology-derived microvessel maps. *Phys Med Biol* 2011; **56**: 2045–57. doi: [10.1088/0031-9155/56/7/009](https://doi.org/10.1088/0031-9155/56/7/009)
89. Mönnich D, Troost EG, Kaanders JH, Oyen WJ, Alber M, Zips D, et al. Correlation between tumor oxygenation and 18F-fluoromisonidazole PET data simulated based on microvessel images. *Acta Oncol* 2013; **32**: 1308–13. doi: [10.3109/0284186X.2013.812796](https://doi.org/10.3109/0284186X.2013.812796)
90. Carlin S, Zhang H, Reese M, Ramos NN, Chen Q, Ricketts SA. A comparison of the imaging characteristics and microregional distribution of 4 hypoxia PET tracers. *J Nucl Med* 2014; **55**: 515–21. doi: [10.2967/jnumed.113.126615](https://doi.org/10.2967/jnumed.113.126615)
91. Peeters SG, Zegers CM, Lieuwes NG, van Elmpt W, Eriksson J, van Dongen GA, et al. A comparative study of the hypoxia PET tracers [¹⁸F]HX4, [¹⁸F]FAZA, and [¹⁸F]FMISO in a preclinical tumor model. *Int J Radiat*

- Oncol Biol Phys* 2015; **91**: 351–9. doi:[10.1016/j.ijrobp.2014.09.045](https://doi.org/10.1016/j.ijrobp.2014.09.045).
92. Trigonis I, Koh PK, Taylor B, Tamal M, Ryder D, Earl M, et al. Early reduction in tumour [¹⁸F]fluorothymidine (FLT) uptake in patients with non-small cell lung cancer (NSCLC) treated with radiotherapy alone. *Eur J Nucl Med Mol Imaging* 2014; **41**: 682–93. doi: [10.1007/s00259-013-2632-3](https://doi.org/10.1007/s00259-013-2632-3)
 93. Hoeben BA, Troost EG, Span PN, van Herpen CM, Bussink J, Oyen WJ, et al. 18F-FLT PET during radiotherapy or chemoradiotherapy in head and neck squamous cell carcinoma is an early predictor of outcome. *J Nucl Med* 2013; **54**: 532–40. doi: [10.2967/jnumed.112.105999](https://doi.org/10.2967/jnumed.112.105999)
 94. Elsässer-Beile U, Reischl G, Wiehr S, Bühler P, Wolf P, Alt K, et al. PET imaging of prostate cancer xenografts with a highly specific antibody against the prostate-specific membrane antigen. *J Nucl Med* 2009; **50**: 606–11. doi: [10.2967/jnumed.108.058487](https://doi.org/10.2967/jnumed.108.058487)
 95. Afshar-Oromieh A, Zechmann CM, Malcher A, Eder M, Eisenhut M, Linhart HG, et al. Comparison of PET imaging with a (68)Ga-labelled PSMA ligand and (18)F-choline-based PET/CT for the diagnosis of recurrent prostate cancer. *Eur J Nucl Med Mol Imaging* 2014; **41**: 11–20. doi: [10.1007/s00259-013-2525-5](https://doi.org/10.1007/s00259-013-2525-5)
 96. Niyazi M, Geisler J, Siefert A, Schwarz SB, Ganswindt U, Garny S, et al. FET-PET for malignant glioma treatment planning. *Radiother Oncol* 2011; **99**: 44–8. doi: [10.1016/j.radonc.2011.03.001](https://doi.org/10.1016/j.radonc.2011.03.001)
 97. Rieken S, Habermehl D, Giesel FL, Hoffmann C, Burger U, Rief H, et al. Analysis of FET-PET imaging for target volume definition in patients with gliomas treated with conformal radiotherapy. *Radiother Oncol* 2013; **109**: 487–92. doi: [10.1016/j.radonc.2013.06.043](https://doi.org/10.1016/j.radonc.2013.06.043)
 98. Grosu AL, Weber WA, Riedel E, Jeremic B, Nieder C, Franz M, et al. L-(methyl-11C) methionine positron emission tomography for target delineation in resected high-grade gliomas before radiotherapy. *Int J Radiat Oncol Biol Phys* 2005; **63**: 64–74. doi: [10.1016/j.ijrobp.2005.01.045](https://doi.org/10.1016/j.ijrobp.2005.01.045)
 99. Townsend DW, Beyer T. A combined PET/CT scanner: the path to true image fusion. *Br J Radiol* 2002; **75**: S24–30. doi: [10.1259/bjr.75.suppl_9.750024](https://doi.org/10.1259/bjr.75.suppl_9.750024)
 100. Disselhorst JA, Bezrukov I, Kolb A, Parl C, Pichler BJ. Principles of PET/MR imaging. *J Nucl Med* 2014; **55**(Suppl. 2): 2S–10. doi: [10.2967/jnumed.113.129098](https://doi.org/10.2967/jnumed.113.129098)
 101. Dalah E, Moraru I, Paulson E, Erickson B, Li XA. Variability of target and normal structure delineation using multimodality imaging for radiation therapy of pancreatic cancer. *Int J Radiat Oncol Biol Phys* 2014; **89**: 633–40. doi: [10.1016/j.ijrobp.2014.02.035](https://doi.org/10.1016/j.ijrobp.2014.02.035)
 102. Houweling AC, Wolf AL, Vogel WV, Hamming-Vrieze O, van Vliet-Vroegindeweij C, van de Kamer JB, et al. FDG-PET and diffusion-weighted MRI in head-and-neck cancer patients: implications for dose painting. *Radiother Oncol* 2013; **106**: 250–4. doi: [10.1016/j.radonc.2013.01.003](https://doi.org/10.1016/j.radonc.2013.01.003)
 103. Groenendaal G, van den Berg CA, Korporaal JG, Philippens ME, Luijten PR, van Vulpen M, et al. Simultaneous MRI diffusion and perfusion imaging for tumor delineation in prostate cancer patients. *Radiother Oncol* 2010; **95**: 185–90. doi: [10.1016/j.radonc.2010.02.014](https://doi.org/10.1016/j.radonc.2010.02.014)
 104. van Elmpt W, Das M, Hüllner M, Sharifi H, Zegers CM, Reymen B, et al. Characterization of tumor heterogeneity using dynamic contrast enhanced CT and FDG-PET in non-small cell lung cancer. *Radiother Oncol* 2013; **109**: 65–70. doi: [10.1016/j.radonc.2013.08.032](https://doi.org/10.1016/j.radonc.2013.08.032)
 105. Iizuka Y, Matsuo Y, Umeoka S, Nakamoto Y, Ueki N, Mizowaki T, et al. Prediction of clinical outcome after stereotactic body radiotherapy for non-small cell lung cancer using diffusion-weighted MRI and (18)F-FDG PET. *Eur J Radiol* 2014; **83**: 2087–92. doi: [10.1016/j.ejrad.2014.07.018](https://doi.org/10.1016/j.ejrad.2014.07.018)
 106. Lambrecht M, Deroose C, Roels S, Vandecaveye V, Penninckx F, Sagaert X, et al. The use of FDG-PET/CT and diffusion-weighted magnetic resonance imaging for response prediction before, during and after preoperative chemoradiotherapy for rectal cancer. *Acta Oncol* 2010; **49**: 956–63. doi: [10.3109/0284186x.2010.498439](https://doi.org/10.3109/0284186x.2010.498439)
 107. Alber M, Thorwarth D. Multi-modality functional image guided dose escalation in the presence of uncertainties. *Radiother Oncol* 2014; **111**: 354–9. doi: [10.1016/j.radonc.2014.04.016](https://doi.org/10.1016/j.radonc.2014.04.016)
 108. Parmar C, Rios Velazquez E, Leijenaar R, Jermoumi M, Carvalho S, Mak RH, et al. Robust Radiomics feature quantification using semiautomatic volumetric segmentation. *PLoS One* 2014; **9**: e102107. doi: [10.1371/journal.pone.0102107](https://doi.org/10.1371/journal.pone.0102107)
 109. Aerts HJ, Velazquez ER, Leijenaar RT, Parmar C, Grossmann P, Cavalho S, et al. Decoding tumour phenotype by noninvasive imaging using a quantitative radiomics approach. *Nat Commun* 2014; **5**: 4006. doi: [10.1038/ncomms5006](https://doi.org/10.1038/ncomms5006)
 110. Thorwarth D, Beyer T, Boellaard R, de Ruyscher D, Grgic A, Lee JA, et al. Integration of FDG-PET/CT into external beam radiation therapy planning: technical aspects and recommendations on methodological approaches. *Nuklearmedizin* 2012; **51**: 140–53. doi: [10.3413/Nukmed-0455-11-12](https://doi.org/10.3413/Nukmed-0455-11-12)
 111. Paulus DH, Thorwarth D, Schmidt H, Quick HH. Towards integration of PET/MR hybrid imaging into radiation therapy treatment planning. *Med Phys* 2014; **41**: 072505. doi: [10.1118/1.4881317](https://doi.org/10.1118/1.4881317)
 112. Leibfarth S, Mönnich D, Welz S, Siegel C, Schwenzer N, Schmidt H, et al. A strategy for multimodal deformable image registration to integrate PET/MR into radiotherapy treatment planning. *Acta Oncol* 2013; **52**: 1353–9. doi: [10.3109/0284186X.2013.813964](https://doi.org/10.3109/0284186X.2013.813964)
 113. Fortunati V, Verhaart RF, Angeloni F, van der Lugt A, Niessen WJ, Veenland JF, et al. Feasibility of multimodal deformable registration for head and neck tumor treatment planning. *Int J Radiat Oncol Biol Phys* 2014; **90**: 85–93. doi: [10.1016/j.ijrobp.2014.05.027](https://doi.org/10.1016/j.ijrobp.2014.05.027)
 114. Sattler B, Lee JA, Lonsdale M, Coche E. PET/CT (and CT) instrumentation, image reconstruction and data transfer for radiotherapy planning. *Radiother Oncol* 2010; **96**: 288–97. doi: [10.1016/j.radonc.2010.07.009](https://doi.org/10.1016/j.radonc.2010.07.009)
 115. Cheebsumon P, Yaqub M, van Velden FH, Hoekstra OS, Lammertsma AA, Boellaard R. Impact of [¹⁸F]FDG PET imaging parameters on automatic tumour delineation: need for improved tumour delineation methodology. *Eur J Nucl Med Mol Imaging* 2011; **38**: 2136–44. doi: [10.1007/s00259-011-1899-5](https://doi.org/10.1007/s00259-011-1899-5)
 116. Cheebsumon P, van Velden FH, Yaqub M, Frings V, de Langen AJ, Hoekstra OS, et al. Effects of image characteristics on performance of tumor delineation methods: a test-retest assessment. *J Nucl Med* 2011; **52**: 1550–8. doi: [10.2967/jnumed.111.088914](https://doi.org/10.2967/jnumed.111.088914)
 117. Knudtsen IS, van Elmpt W, Ollers M, Malinen E. Impact of PET reconstruction algorithm and threshold on dose painting of non-small cell lung cancer. *Radiother Oncol* 2014; **113**: 210–14. doi: [10.1016/j.radonc.2014.09.012](https://doi.org/10.1016/j.radonc.2014.09.012)
 118. Schakel T, Hoogduin JM, Terhaard CH, Philippens ME. Diffusion weighted MRI in head-and-neck cancer: geometrical accuracy. *Radiother Oncol* 2013; **109**: 394–7. doi: [10.1016/j.radonc.2013.10.004](https://doi.org/10.1016/j.radonc.2013.10.004)
 119. Intven M, Reerink O, Philippens ME. Repeatability of diffusion-weighted imaging in rectal cancer. *J Magn Reson Imaging* 2014; **40**: 146–50. doi: [10.1002/jmri.24337](https://doi.org/10.1002/jmri.24337)